The Highly Exposed Loop Region in Mammalian Purple Acid Phosphatase Controls the Catalytic Activity

Enrico G. Funhoff,[a] Corné H. W. Klaassen,[b] Bart Samyn,[c] Jozef Van Beeumen,[c] and Bruce A. Averill*[a]

Recombinant human purple acid phosphatase (recHPAP) provides a convenient experimental system for assessing the relationship between molecular structure and enzymatic activity in mammalian purple acid phosphatases (PAPs). recHPAP is a monomeric protein with properties similar to those of uteroferrin (Uf) and other PAPs isolated as single polypeptide chains, but its properties differ significantly from those of bovine spleen PAP (BSPAP) and other PAPs isolated as proteolytically "clipped" forms. Incubation of recHPAP with trypsin results in proteolytic cleavage in an exposed region near the active site. The product is a tightly associated two-subunit protein whose collective spectroscopic and kinetics properties resemble those of BSPAP. These results demonstrate that the differences in spectroscopic and kinetics properties previously reported for mammalian PAPs are the result of proteolytic cleavage. Mass spectrometry shows that a three-residue segment, D-V-K, within the loop region is excised by trypsin. This finding suggests that important interactions between residues in the excised loop and one or more of the groups that participate in catalysis are lost or altered upon proteolytic cleavage. Analysis of available structural data indicates that the most important such interaction is that between Asp 146 in the exposed loop and active-site residues Asn 91 and His 92. Loss of this interaction should result in both an increase in the Lewis acidity of the Fe^{II} ion and an increase in the nucleophilicity of the Fe^{III}-bound hydroxide ion. Proteolytic cleavage thus constitutes a potential physiological mechanism for regulating the activity of PAP in vivo.

Introduction

Purple acid phosphatases (PAPs)[**] are metalloenzymes that catalyze the hydrolysis of phosphoric acid monoesters; they have an $\alpha\beta$-type structure that contains a metallophoesterase signature sequence motif.[1, 2] PAPs are characterized by their purple color, their ability to efficiently hydrolyze unactivated phosphoric acid esters, their pH optimum in the acidic region, and their insensitivity to tartrate inhibition.[3–6]

PAPs, also referred to as tartrate-resistant acid phosphatases (TRAPs) or type-5 acid phosphatases (EC 3.1.3.2),[7] have been isolated from mammalian sources such as bovine spleen (BSPAP), porcine uterine fluids (Uf), rat spleen and bone, and human tissues. Similar enzymes are present in plants (e.g., red kidney beans (KBPAP), sweet potatoes, and *Arabidopsis thaliana*) and in microorganisms.[6] The subunit molecular mass of PAP from various sources ranges from approximately 55 kDa for the plant enzymes to 35 kDa for the mammalian enzymes. The primary structures of mammalian PAPs are highly homologous; for example, BSPAP and Uf exhibit 84 – 90% sequence identity to the human enzyme.[8–10]

Of the mammalian PAPs, those from bovine spleen and porcine uterine fluids are the best characterized. The enzymatically active form contains a mixed-valent binuclear cluster at the active site, in which a high-spin Fe^{II} ion and a high-spin Fe^{III} ion are antiferromagnetically coupled to give an $S = 1/2$ ground state.[11–13] The one-electron oxidized ($Fe^{III}Fe^{III}$) form is also antiferromagnetically coupled ($S = 0$ ground state); it is essentially inactive, with $\leq 10\%$ of the activity of the mixed-valent

[a] B. A. Averill, E. G. Funhoff
E. C. Slater Institute
Biocentrum Amsterdam
University of Amsterdam
Plantage Muidergracht 12, 1018 TV Amsterdam (The Netherlands)
Fax: (+31) 20-5255124
E-mail: BAA@chem.uva.nl

[b] C. H. W. Klaassen
Department of Biochemistry
Institute of Cellular Signalling
University of Nijmegen
Postbox 9101, 6500 HB Nijmegen (The Netherlands)

[c] B. Samyn, J. Van Beeumen
Department of Biochemistry, Physiology and Microbiology
Laboratorium of Protein Biochemistry and Protein Engineering
University of Gent
K. L. Ledeganckstraat 35, 9000 Gent (Belgium)

Supporting information for this article is available on the WWW under http://www.chembiochem.com or from the author.

[**] For abbreviations see ref. [64].

form. This residual activity has been shown to be due to the presence of small amounts of an $Fe^{III}Zn^{II}$ form.[14] Both the divalent and trivalent metal ions in Uf and BSPAP can be replaced by, for example, Zn^{II} or Co^{II} and Ga^{III} or Al^{III}, respectively, resulting in active enzymes that exhibit relatively minor differences in kinetics parameters and inhibition constants.[13, 15–19]

The first X-ray crystal structure of a PAP, the 110-kDa dimer from kidney bean, showed the presence of an FeZn center coordinated by three histidines, two aspartates, a tyrosine, and an asparagine.[20] In addition, three histidines were proposed to act as acidic or basic groups that interact with the substrate during catalysis. The X-ray crystal structures of two Ser/Thr-specific protein phosphatases, protein phosphatases 1 (PP1)[21, 22] and 2B (calcineurin),[23, 24] show the presence of very similar binuclear metal centers in which the same amino acids are coordinated to the metal ions with virtually identical geometries. The only exception is the replacement of the tyrosinate ligand present in the PAPs by a coordinated water molecule in the PPs, accounting for the absence of the purple color in the latter. Very recently, three additional structures of mammalian PAPs have been published, those from rat bone (at 2.7 Å[25] and 2.2 Å resolution[27]) and from porcine uterine fluids (at 1.5 Å resolution[26]). These structures show that the amino acids coordinated to the binuclear center and the secondary structure of the mammalian PAPs are identical to those of the plant PAPs and the PPs. A disulfide bond is present in both the Uf structure and the 2.7-Å rat bone PAP structure, but is apparently absent in the 2.2-Å rat bone PAP structure. In all three structures the proteins are glycosylated on Asn 97.[25–27]

The mammalian PAPs studied to date are quite similar in their spectroscopic and catalytic properties. All exhibit a $g_{av} = 1.74$ rhombic EPR spectrum, a broad visible absorbance band at ca. 550 nm, and a pH optimum in the acidic region (4.9–6.3). Surprisingly, however, PAPs from different sources and preparations exhibit rather large differences in their catalytic activity, with reported turnover numbers ranging from 200 to 3000 s^{-1}. The origin of these differences has long been unclear, although suggestive evidence has been presented linking higher enzymatic activity with proteolysis of the protein. For example, the activity of both bovine spleen PAP and Uf has been shown to increase upon incubation with proteases,[28] presumably due to cleavage of the polypeptide. Similar increases in activity, accompanied by a shift in pH optimum, have been reported upon proteolysis of recombinant rat PAP (recRPAP),[29, 30] while recombinant human PAP (recHPAP) is also suspected to be sensitive to proteolysis.[31] The loop that is apparently subject to proteolysis is a highly antigenic portion of the polypeptide that is present in the three-dimensional structure of Uf[26] and in one of the rat bone PAP structures,[27] but which could not be resolved in the other rat bone PAP structure.[25] Why proteolysis of this loop affects the catalytic activity of mammalian PAPs is, however, not known. Because published studies have utilized different enzyme preparations and sources, the extent and location of proteolysis have been difficult to ascertain and/or control. In addition, the system for which the proteolysis process is best characterized (recRPAP) is among the least well-characterized in terms of spectroscopic and kinetic studies. Conversely,

the two benchmarks for spectroscopic and kinetics studies have been BSPAP, which is normally isolated in a proteolytically cleaved form, and Uf, which is isolated as a single polypeptide of 36 kDa. Unfortunately, no proteolysis or site-directed mutagenesis studies have been reported for these enzymes.

We have utilized recHPAP as a model system with which to study the correlation between proteolysis and the catalytic and spectroscopic properties of PAP. recHPAP has been isolated, and both the intact enzyme and its proteolytically cleaved form have been characterized. Our results indicate that the differences in kinetics and spectroscopic properties reported for mammalian PAPs are due to variations in the extent of proteolytic cleavage in an exposed loop near the active site. A molecular basis for the effect of proteolytic cleavage on the catalytic and spectroscopic properties of the enzyme is presented. These findings are consistent with the use of proteolytic activation as a physiological mechanism for regulation of PAP activity.

Results

Production, purification, and proteolytic activation of recHPAP

Production of recHPAP with Sf9 cells from *Spodoptera frugiperda* resulted in recHPAP expression levels of 1–2 U mL^{-1} at six days post infection (dpi). Purification of the protein was accomplished by a combination of the procedures of Hayman and Cox[34] and Vincent et al.[40] Phosphocellulose (P11) adsorption was used to reduce the volume, followed by hydrophobic interaction chromatography, cation exchange chromatography and size exclusion chromatography. This procedure yielded ca. 15 mg pure protein from a 10-L batch; Western blot analysis showed a band at ca. 36 kDa with some heterogeneity due to variable glycosylation (see below). The protein was stored at $-20\,^{\circ}$C for several months without any evidence of cleavage, as tested by SDS-PAGE.

Both BSPAP and recRPAP are known to be susceptible to proteolytic activation by trypsin.[28, 29] To examine proteolytic activation of recHPAP, trypsin was used to cleave the 36-kDa protein. As shown by SDS-PAGE, the resulting protein consisted of two fragments with masses of 20 kDa and 16 kDa (see Figure S1 in the Supporting Information).

Mass spectrometry and sequencing

Reversed-phase (RP) HPLC, mass spectrometry, and N- and C-terminal sequencing were used to discriminate between single cleavage within the loop and partial or complete removal of the loop and to determine the site(s) of cleavage. RP-HPLC analysis of both monomeric and cleaved recHPAP resulted in chromatograms with a single peak with the same retention time. This indicated that after cleavage the two fragments were still connected through a cysteine bridge (residues 142 and 200 in the human sequence[10]). After denaturation of the trypsin-cleaved protein and reduction of the disulfide bridge with DTT,

two peaks were observed, consistent with cleavage to give two fragments.

A molecular mass of $36\,264.8 \pm 1.3$ Da was found for monomeric recHPAP, which does not correspond to the calculated mass of 34328.9 Da (Table 1). Previous deglycosylation experi-

Enzyme	Mass [Da][a]	Theoretical mass [Da]	C terminus	N terminus
native recHPAP	36264.8 (1.3)	34328.9		A-T-P-A
cleaved recHPAP	35947.2 (8.1)	34346.9	L(?)-V-K	A-T-P-A
				L-A-R-T
large fragment	19486.1 (1.0)	17896.2		A-T-P-A
small fragment	16454.5 (0.5)	16452.8		L-A-R-T

[a] Numbers in parentheses are standard deviation values.

ments with recombinant human and rat PAP indicate that the difference (1935.9 Da) is almost certainly due to glycosylation.[34, 44] Other minor peaks in the mass spectrum could be explained by heterogeneity of glycosylation of recHPAP (e.g., the presence of various extra monosaccharides such as deoxyhexose and hexuronic acid) as suggested by SDS-PAGE. After cleavage with trypsin, electrospray ionization mass spectrometry (ESI-MS) showed that the mass of the two-subunit protein was $35\,947.2 \pm 8.1$ Da. A fragment with a mass of 335.6 ± 8.1 Da is thus removed during proteolysis. Quadrupole time-of-flight (Q-TOF) MS analysis of the reduced fractions yielded a large fragment with a mass of $19\,486.1 \pm 1.0$ Da and a smaller fragment with a mass of $16\,454.5 \pm 0.5$ Da. These results were confirmed by ESI-MS analysis. The calculated masses of the large and small fragments are 17896.2 and 16452.8 Da, respectively; thus the small fragment is not modified. The difference of 335.6 Da between the native and the nonreduced trypsin-cleaved protein is therefore a result of the modification of the large fragment. It can be explained by a second cleavage between Arg 151 and Asp 152, resulting in the loss of the last three amino acids of the C terminus of the large fragment, D-V-K (calculated mass 342.4 Da).

During Edman degradation of the RP-LC eluate (nonreduced), two N-terminal sequences were observed. The first sequence, A-T-P-A, corresponded to the N terminus of the enzyme after posttranslational processing. The second sequence was L-A-R-T-Q, corresponding to the amino acids starting at position 161. C-terminal sequence analysis of the sample indicated only one (very weak) sequence, (Leu?)-Val-Lys (0.01%). The C-terminal

sequence of the small subunit was not observed since it ends with Pro, a residue that precludes C-terminal sequence analysis.[61] After denaturation and reduction neither of the fragments yielded any sequence information. This is in agreement with the second cleavage, since Arg as the C-terminal amino acid also precludes C-terminal sequence analysis.

Enzymatic parameters of intact and cleaved recHPAP

Previously reported specific activities for recHPAP vary from 190 U mg^{-1} at pH 5.6[34] to 350 U mg^{-1} at pH 4.9.[31] To gain insight into the origin of the differences between the intact and cleaved protein, k_{cat} versus pH profiles were measured. The k_{cat} versus pH profile of the intact protein showed a symmetric bell-shaped curve with an optimum at pH 5.5 (Figure 1). At 22 °C the intact mixed-valent recHPAP had a specific activity of 520 U mg^{-1}, with a K_M value of 4.8 mM for the substrate p-NPP at its optimal pH (Table 2). At the often used pH of 6.0, the activity was lower (440 U mg^{-1}) and the K_M value higher (8.6 mM). The pH dependencies were analyzed according to a rapid-equilibrium diprotic model.[41, 42] The following expressions were derived for the observed values of k_{cat} defined as in Equation (1), and k_{cat}/K_M as
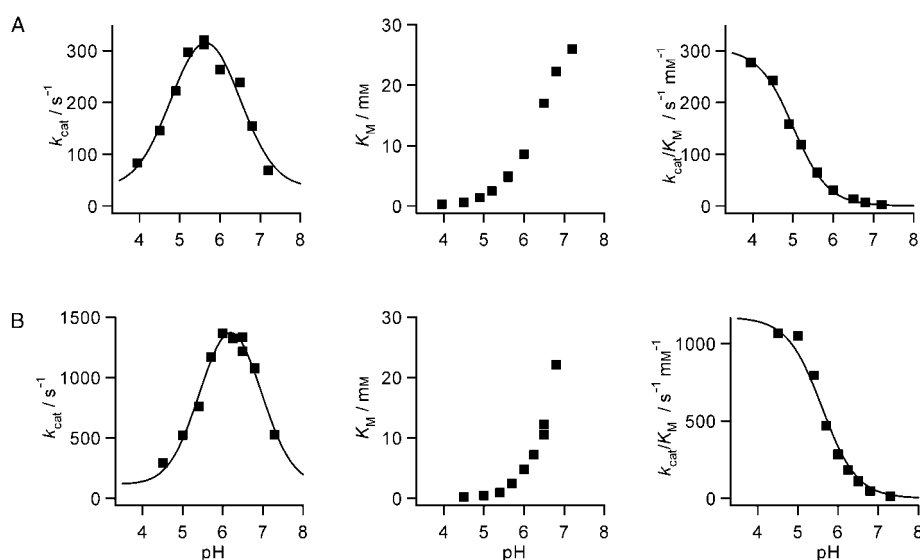

Figure 1. *Dependencies of* k_{cat}, k_{cat}/K_M, *and* K_M *on pH for monomeric (A) and cleaved recHPAP (B) with* p-NPP *as substrate at 22 °C. The lines represent fits of* k_{cat} *and* k_{cat}/K_M *to the rapid-equilibrium diprotic model.*

Table 2. *Kinetics constants of monomeric and cleaved recHPAP with* p-NPP.[a]

Enzyme	pH$_{opt}$	K_M [mM]	k_{cat} [s^{-1}]	p$K_{ES,1}$[b]	p$K_{ES,2}$[b]	p$K_{E,2}$[c]
recHPAP$_{mono,red}$	5.5	4.8	310	4.6	6.7	5.0
recHPAP$_{cleaved,red}$	6.2	7.2	1250	5.5	6.9	5.6

[a] k_{cat} is defined as the number of substrate molecules hydrolyzed per enzyme molecule per second, p$K_{ES,1}$ and p$K_{ES,2}$ as a deprotonation/protonation event of a group of the enzyme – substrate complex, p$K_{E,2}$ as a deprotonation/protonation event of a group on the enzyme, and K_S as the dissociation constant of the ES complex. [b] Obtained from a fit of k_{cat} as a function of pH. [c] Obtained from a fit of k_{cat}/K_M as a function of pH with p$K_{E,1} < 2$. Assays were performed at 22 °C in a buffer containing 100 mM MES, 10 mM Na-K tartrate, 300 mM KCl, 6.7 mM Na ascorbate, and 0.37 mM $(NH_4)_2Fe(SO_4)_2$.

defined in Equation (2), assuming that all equilibria are fast compared to k_{cat} (see Table 2 for definitions).

$$k_{cat(obs)} = k_{cat}/(1+[H^+]/K_{ES,1}+K_{ES,2}/[H^+]) \quad (1)$$

$$k_{cat(obs)}/K_{M(obs)} = k_{cat}/K_S(1+[H^+]/K_{E,1}+K_{E,2}/[H^+]) \quad (2)$$

Fitting of the k_{cat} dependencies resulted in the pK_a values given in Table 2. The oxidized protein typically had a residual activity of 5–10%. The K_M value and the pH optimum were similar to those of the intact mixed-valent protein.

Cleavage with trypsin resulted in an almost fivefold increase in activity at pH 6 (420 versus 2100 U mg^{-1}; Table 2). In addition, the pH optimum shifted from 5.5 to 6.2. Analysis of the data indicated that p$K_{ES,1}$ increased from 4.6 to 5.5, while the effect on the p$K_{ES,2}$ value was less pronounced (6.7 versus 6.9). The k_{cat}/K_M versus pH data could be fitted by using a single pK_a value (p$K_{E,2}$), but the lack of data at low pH suggests that this result should be interpreted with some care. Nonetheless, it is clear that a significant shift in p$K_{E,2}$ occurs (5.0 versus 5.6). The K_M value for the cleaved protein is also lower than that of the intact protein at pH 6.0 (4.8 versus 8.5 mM).

Spectroscopic characterization of intact and cleaved recHPAP

In order to determine if the change in kinetics properties upon cleavage could be caused by a change in secondary structure, circular dichroism (CD) measurements were performed on the intact and cleaved forms of recHPAP. The spectra of both forms exhibit strong negative ellipticities with shoulders at 210 and 218 nm. The CD spectra of the intact and cleaved proteins are virtually identical to one another in both the mixed-valent and oxidized states, suggesting that neither proteolytic cleavage nor oxidation of the dinuclear iron center is accompanied by significant structural rearrangements (see Figure S2 in the Supporting Information). Results of quantitation of the secondary structure are summarized in Table 3, which shows that approximately 15% random-coil structure is present in all forms studied. No significant differences between intact and cleaved recHPAP were found, although the latter apparently had slightly lower α-helix (35 versus 27%) and higher β-turn (15 versus 25%) contents. In the oxidized state, however, virtually identical α-helix, β-sheet and -turn, and random-coil contents were observed for both the intact and cleaved forms. In addition, the optical spectra of both intact and cleaved recHPAP were identical, showing a tyrosine-to-Fe^{III} charge transfer band at

520 nm that shifted to lower energy (550 nm) upon oxidation with H_2O_2.

The large changes in pK_a value upon cleavage observed in the kinetics studies indicate that there must be a significant difference between the intact and cleaved proteins. Because EPR spectroscopy is a very sensitive method that specifically probes structural changes at the diiron site, EPR spectra of both the intact and cleaved proteins were obtained. The intact mixed-valent recHPAP exhibits a typical $S = 1/2$ rhombic spectrum, with apparent g values of 1.94, 1.73, and 1.56 (Figure 2A). This spectrum is virtually identical to that reported for Uf,[43] which is isolated as an intact 36-kDa polypeptide. In contrast, the proteolytically cleaved mixed-valent protein gave a rhombic spectrum with apparent g values of 1.86, 1.73, and 1.58 (Figure 2D). This spectrum is very similar to that of BSPAP, which is isolated as a proteolytically cleaved form.
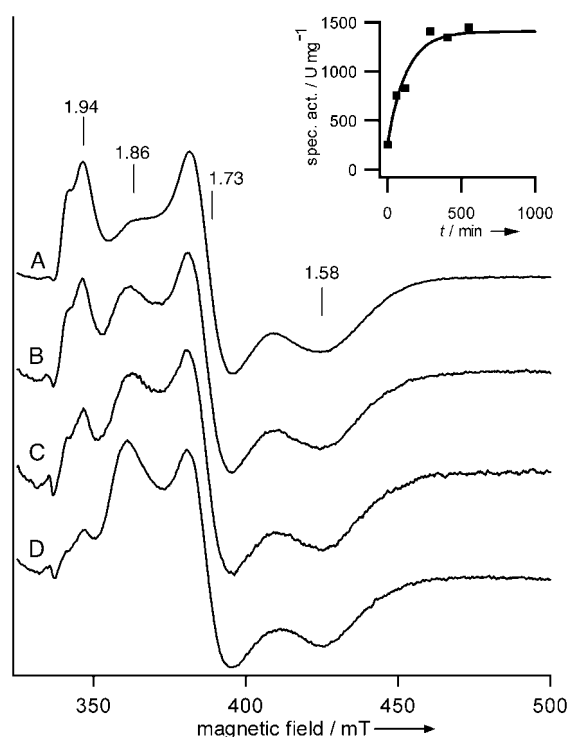

Figure 2. Monitoring tryptic cleavage of recHPAP by EPR spectroscopy. Spectra were recorded at a specific activity of 365 (A), 965 (B), 1280 (C), and 1500 U mg^{-1} (D). The amplitudes were corrected for instrument gain and protein concentration. EPR conditions: microwave power = 20 mW, microwave frequency = 9.42 GHz, modulation = 12.7 G at 100 kHz, T = 4.3 K. The insert shows the increase in specific activity (spec. act.) with time.

In order to confirm that the changes in EPR spectra were indeed due to cleavage and correlated with changes in specific activity, a large-scale proteolysis experiment was monitored by EPR spectroscopy (Figure 2). The spectra clearly show that the $g = 1.94$ feature disappears with concomitant appearance of a signal at $g = 1.86$, and that the spectral changes parallel the increase in specific activity.

Table 3. Average secondary-structure content of recHPAP as determined from CD spectra.[a]

Enzyme	λ_{max} [nm]	α helix [%]	β sheet [%]	β turn [%]	random coil [%]
recHPAP$_{mono,red}$	520	35 (3)	35 (6)	15 (7)	15 (5)
recHPAP$_{cleaved,red}$	520	27 (3)	33 (8)	25 (3)	15 (12)
recHPAP$_{mono,ox}$	550	32 (2)	35 (5)	17 (5)	16 (3)
recHPAP$_{cleaved,ox}$	555	34 (4)	37 (9)	19 (6)	10 (7)
[a] Numbers in parentheses are standard deviation values.					

Discussion

Like recHPAP, Uf and recRPAP are isolated as intact polypeptides with a molecular mass of ca. 36 kDa. Compared to PAPs such as BSPAP and the rat bone and spleen PAPs, which are isolated as proteins consisting of two fragments of molecular mass of 20 and 16 kDa, the former exhibit: i) lower specific activity ($k_{cat} \approx$ 300 s^{-1}); ii) a more acidic pH optimum; and iii) a more rhombic EPR spectrum, with apparent *g* values of ca. 1.94, 1.73, and 1.58.[7, 13, 31, 34, 40, 43–47]

The large differences in specific activity reported for mammalian PAPs appear to be related to the presence or absence of proteolytic cleavage. Treatment of monomeric BSPAP, Uf, and recRPAP with proteases such as trypsin, papain, or cathepsin has been reported to result in the formation of a two-subunit protein with a significant increase in activity[28, 29] and a shift in pH optimum.[29] In the present study, we attempted to clarify the relationship between proteolytic cleavage, kinetics properties, and spectroscopic characteristics by using a representative recombinant mammalian PAP.

Treatment of recHPAP with trypsin results in a cleaved protein with an increased specific activity, which is comparable to that of recRPAP treated with cysteine proteases.[29] Although cleavage by trypsin is highly unlikely to be physiologically relevant, trypsin was used in these experiments because of the presence of well-defined trypsin cleavage sites and the activation of BSPAP and Uf by trypsin reported earlier.[28] Physiologically relevant proteases are the cathepsins, cysteine proteases that are present in the same cells as PAP.[29] For recRPAP and BSPAP, the N-terminal sequences of the small subunit are D-L-G-V-A-R-T-Q and N-L-A-M-A-R-T-Q, respectively, while the N-terminal sequence of the small subunit of the recombinant human protein is shorter by three amino acids, L-A-R-T-Q. This would imply that the precise site of cleavage has an important effect on the specific activity. As shown in Table 4, cleavage at the end of the loop, in or near the sequence A-R-T-Q, seems to produce proteins with higher specific activity than cleavage upstream of this sequence.[28, 29] Mass spectrometry indicates that three amino acids at the C terminus of the large fragment in recHPAP are removed by

trypsin. The mass of the small fragment produced by trypsin cleavage is the same as the calculated mass of 16 452 Da. The difference of 335.6 Da found between the monomeric and nonreduced cleaved recHPAP must therefore be due to proteolytic processing of the larger subunit. Within experimental error, this difference is equal to the mass of D-V-K (calculated mass 342.7 Da), which are the C-terminal amino acids of the larger fragment. A V-K C terminus was found, but corresponded to only 0.01 % of the sample. The C termini of both the small and large subunit are known to preclude C-terminal sequence analysis, and therefore, they were not detected.[61] Removal of these three amino acids should weaken or abolish the interaction of the loop region with the active-site residues, with a concomitant increase in activity. This would explain why almost no increase in activity is found upon trypsin cleavage of recRPAP, for which only one cleavage site is available; presumably the resulting amino acid "tail" is held in place by noncovalent forces. When papain is used, however, six amino acids between Glu 154 and Gly 160 (Table 4), are removed, again leading to complete loss of the interaction of the exposed loop with the active site and an increase in enzymatic activity. The variability of cleavage products with proteases is supported by the finding of Ljusberg et al. that SDS-PAGE analyis of trypsin- and papain-digested recRPAP shows different N-terminal fragment masses.[29]

The EPR spectrum of intact recHPAP resembles those of Uf and intact recRPAP. All of these proteins consist of a single polypeptide chain with a molecular mass of ca. 36 kDa, and in their mixed-valent state all exhibit rhombic EPR spectra with apparent *g* values around 1.94, 1.73, and 1.58.[44, 45] Upon proteolytic cleavage, g_x shifts to 1.86, resulting in a spectrum which resembles that of BSPAP.[28, 46, 48] The λ_{max} value of recHPAP (520 nm) is not affected by proteolytic cleavage, which suggests that cleavage does not affect the position or orientation of the tyrosine ligand. A change in the interaction of the metal ion(s) with a water molecule or in the interaction of the metal ligands with other amino acids upon cleavage could, however, account for the observed differences in EPR spectra. High-salt BSPAP (i.e. BSPAP prepared under high-salt buffer conditions; $\lambda_{max} =$ 536 nm) constitutes an apparent contradiction to this correlation, in that the EPR spectrum reported for intact BSPAP is similar to that of the cleaved form.[28]

Compared to Uf, which exhibits a bell-shaped pH profile with an optimum at 4.9 and p$K_{a,app}$ values of about 4 and 5.2,[49] BSPAP has a higher pH optimum (6.2) with pK_a values of 5.4 and 7.5.[42] Merkx et al. suggested that the reported differences in pH optima between the mammalian PAPs was an artifact resulting from the fact that in most studies the pH profiles were measured under nonsaturating substrate concentrations, leading to a pH profile with a lower pH optimum and shifted pK_a values.[42] We therefore measured k_{cat} as a function of pH for the recombinant human protein before and after proteolytic cleavage. The resulting pH profiles clearly show that the observed difference in pH optima is not artifactual, but reflects real differences in the properties of the enzyme. Fits of the k_{cat} versus pH data to a rapid-equilibrium model allowed extraction of the corresponding pK_a values for the two forms. Both pK_a values increase upon cleavage, p$K_{ES,2}$ by only 0.2 pH units and p$K_{ES,1}$ by almost one full

Table 4. Sequence alignment of mammalian PAPs including their reported cleavage site and corresponding specific activity (U mg^{-1}) after proteolytic digestion.[a]

Enzyme source	Sequence
pig	145S D D F V S Q Q P E R P R N L A L A R T Q L
rat[b]	145S D D F V S Q Q P E M P R D L G V A R T Q L
	↑ T 320 ↑ P 1410 ↑ N 1640
human[c]	145S D D F L S Q Q P E R P R D V K L A R T Q L
	↑ (T?) ↑ T 2230
bovine[d]	N L A M A R T Q
	↑ T 1200 ↑ T 2770

[a] T = trypsin, P = papain, N = native (as isolated). [b] From ref. [29]. [c] From ref. [10] and this work. [d] From ref. [28] and ref. [18].

pH unit. In addition, the k_{cat}/K_M versus pH profile shows that $pK_{E,2}$ increases by 0.6 units upon cleavage. The value of $pK_{E,2}$ probably corresponds to a group in the free enzyme that must be protonated in order for the enzyme to bind substrate, possibly one of the conserved histidine residues near the active site. The acidic pK_a value in the k_{cat} versus pH profile has been attributed to a water molecule coordinated to the Fe^{III} ion in the enzyme–substrate complex,[19, 42, 50] but the identity of the group giving rise to $pK_{ES,2}$ remains unclear. The magnitude of the observed change in $pK_{ES,1}$ suggests that proteolytic cleavage causes a significant change in the interactions between the protein and a coordinated water molecule. This conclusion is in agreement with the change in EPR spectrum, as discussed earlier.

In addition to the effect of proteolytic cleavage upon the pH dependence of the catalytic properties, the activity of the enzyme at its optimum pH is also affected by proteolysis. Our results show that proteolysis of recHPAP with trypsin increases the value of k_{cat} by a factor of about four, while K_M is not affected. For recRPAP, however, a decrease in K_M is observed upon proteolysis, and consequently the catalytic efficiency of the cleaved enzyme as judged by the k_{cat}/K_M criterion is higher. In this case the assays were performed at one standard pH value and not at the optimal pH value for each species.[29] Why proteolytic cleavage of an exposed loop on the surface of the protein should have such a large effect upon the catalytic properties of the enzyme constitutes an important problem.

The simplest explanation for the increase in enzymatic activity upon proteolysis is a steric one, in which cleavage or removal of the loop increases accessibility of the active site to the substrate. This explanation is unlikely to be correct, however, because the X-ray crystal structures in which the loop is resolved show no evidence that it blocks access to the active site. Further, such an explanation would predict a larger effect on K_M than on k_{cat}, which is the reverse of what is observed. Finally, it is difficult to see how an increase in active-site accessibility would result in the similar changes in pK_a values and EPR spectra that are observed for all PAPs examined to date.

In principle, proteolysis could also induce a protein conformational change, resulting in the observed changes in activity. CD spectroscopy, however, indicates that negligible changes in secondary structure occur upon cleavage (Table 3). These results do not, however, exclude the possibility that smaller differences in the protein structure occur in the vicinity of the active site. A superposition of the active sites of KBPAP, Uf, and recRPAP shows only minimal differences in the active-site region, suggesting that it is highly conserved and not very flexible. An additional result of this work is the finding that the correlation proposed by Vincent et al.[40] between the magnitude of λ_{max} and the percentage of random-coil secondary structure, as is found for "high-salt" and "low-salt" BSPAP,[28, 40, 51, 52] is apparently not applicable to recHPAP.

The crystal structures of two mammalian PAPs in which the loop region is present and well ordered have been reported recently: Uf at 1.5 Å resolution[26] and a second form of rat bone PAP at 2.2 Å resolution.[27] Both structures show that certain residues in the loop between positions 143 and 160 interact with the active site, and suggest a molecular basis for the changes in

catalytic properties that occur upon proteolytic cleavage. Particularly noteworthy are residues Ser 145 and Asp 146, which are situated near the active site with their side chains directed towards the binuclear metal center. In the following discussion, distances cited are for the Uf crystal structure,[26] which has the highest resolution of the mammalian PAP structures, while the residue numbers correspond to the human sequence.[10] Within experimental error, there are no significant differences to the rat bone PAP structure in which the residues of the loop region are resolved.[27]

The interaction between Ser 145 and Asn 91 is not likely to be important in this regard. This residue is resolved in the same position in both rat bone PAP structures, with and without the loop region.[25, 27] Furthermore, the orientation of the serine hydroxy group is not favourable for hydrogen bonding to the NH_2 group of the Asn side chain. Hence, the following discussion focusses on the role of Asp 146.

The carboxylate group of Asp 146 is in very close proximity to Asn 91, with one oxygen atom only 2.9 Å away from the amido nitrogen atom. Similarly, the side-chain oxygen atom of Ser 145 is only 3.2 Å away from the amido nitrogen atom of Asn 91. Both are thus well within hydrogen-bonding distance. The side chain of Asn 91, which is conserved in all PAP and PP sequences, provides one of the ligands to the divalent metal ion site. Although mutagenesis studies aimed at elucidating the role of this residue have not yet been reported for any PAP, such studies have been performed on the closely related PPs,[23, 24, 53] and the results are consistent with an important role for Asn 91 in both substrate binding and catalysis. As shown in Figure 3, Asp 146 should interact strongly with Asn 91, thereby reducing the Lewis acidity of the Fe^{II} ion and leading to a less activated substrate molecule.

The carboxylate group of Asp 146 can also interact with His 92, with a carboxylate oxygen–imidazole nitrogen distance of only 3.6 Å. Similarly, in PP1 and PP2B the histidine corresponding to His 92 is within 5 Å of both metal ions,[21–24] and it has therefore been proposed to be important in catalysis. Site-directed mutagenesis of phage λ PP,[54] in which this residue is also conserved, suggested that this histidine plays a role in base catalysis through the formation of a His-Asp-M^{n+}-H_2O "catalytic tetrad",[54–56] but this has not yet been confirmed by isotope effect studies.[57] The nearby Asp residue in PPs is believed to be involved in catalysis, because site-directed mutagenesis of this residue to Asn or Ala[53, 55, 58] resulted in a pK_a shift to higher pH. Together with the shift in pH, an almost complete loss of activity was found for the PP mutants. Thus, loss of the Asp–His interaction can explain the shift in pH optimum for mammalian PAPs,[28, 29] but not the increase in activity. This suggests that other interactions are also important.

The picture that emerges from this and other studies is that of an enzyme that, in its native form, contains specific interactions that diminish its catalytic activity. Because PAPs are generally located in organelles that are rich in proteases, the possibility arises that at least some organisms and/or tissues utilize these proteases to release the full intrinsic activity of PAP by proteolytic processing. For example, cathepsins B, H, K, and L are capable of cleaving PAP and are present in osteoclasts,[29]
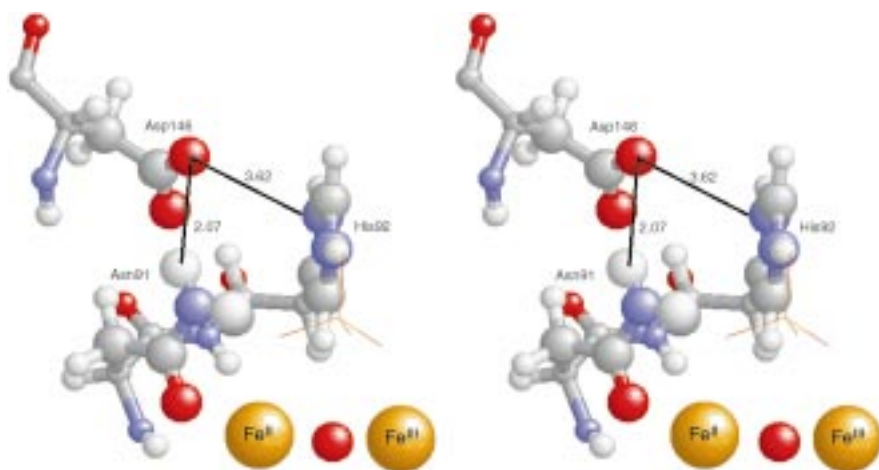
Figure 3. *Stereo view of the interaction of the residues Asn 91, His 92, and Asp 146 of the mammalian purple acid phosphatase Uf (distances are given in Å). The figure was generated with the program RasMol[63] by using the atomic coordinates from the Uf crystal structure[26] (PDB accession code 1Ute).*

which are known to contain PAP. In addition, purification of human osteoclast PAP in the presence of protease inhibitors resulted in a two-subunit PAP[62] similar to BSPAP, suggesting that cleavage was not an artifact of the purification.[28] To date, however, there is no compelling evidence that proteolysis constitutes an important mechanism for controlling PAP activity in vivo. In fact, TCA precipitation of fresh samples of bovine spleen tissue followed by electrophoresis and staining showed that the major form of BSPAP in vivo was the intact 36-kDa polypeptide.[28] These results do not, however, preclude the possibility that differentially processed forms of PAP may be present in different tissues.[7]

In summary, our results strongly suggest that the kinetics and spectroscopic differences reported thus far for mammalian PAPs from different sources are due to variations in the site and extent of proteolytic removal of an exposed loop near the active site of the protein. In particular, proteolytic digestion of several amino acids may result in a flexible C-terminal amino acid tail of the exposed loop. The interaction between a conserved Asp residue in the loop region and active-site residues is suggested to be responsible for the differences in catalytic and spectroscopic properties observed between PAPs isolated as single polypeptide chains and those isolated in proteolytically cleaved form. Site-directed mutagenesis studies of residues in the loop region (e.g., Asp 146) are in progress.

Experimental Section

Materials and instruments: Insect Xpress SFM medium (Bio Whittaker), Phosphocellulose (Whatman), CL-4B phenyl-sepharose (Pharmacia), SP-sepharose (Pharmacia), *p*-NPP (Fluka), trypsin (Sigma), and all other chemicals were of highest purified grade.

Optical spectroscopy was performed on a Carey 50 spectrophotometer. Recombinant protein was produced in a 10-L Applikon bioreactor, controlled by an ADI 1030 Biocontroller, and purified on a

Pharmacia FPLC apparatus. EPR spectra were obtained on an X-band Bruker ECS EPR spectrometer, equipped with an Oxford Instruments ESR900 helium-flow cryostat with an ITC4 temperature controller and an AEG magnetic field calibrator. An AVIV model-I 62ADS CD spectrometer operating at 25 °C and flushed with nitrogen gas was used to measure CD spectra. RP-HPCL was performed with the Pharmacia Biotech SMART system. The alkylated thiohydantoins were identified online by reversed-phase analysis on a Perkin–Elmer 140 C microgradient system. A Perkin–Elmer model 476A protein sequencer operating in the pulsed liquid mode with online PTH analysis was used for N-terminal sequence analysis. C-terminal sequence analysis was performed with a Perkin–Elmer Procise 494C sequencer. For MS analysis a Micromass Q-TOF mass spectrometer with a Protana borosilicate Au/Pd-coated capillary was used.

General procedures: Protein concentrations during purification were determined according to Bradford.[32] The concentration of purified enzyme was determined by measuring the absorption of the tyrosinate-to-Fe^{III} charge transfer band at 520 nm ($\varepsilon = 4080\,M^{-1}\,cm^{-1}$). SDS-PAGE under reducing conditions was performed with 15% gels according to Laemmli.[33] All samples for EPR spectroscopy contained 20% (v/v) glycerol.

Large-scale production of recombinant protein: Sf9 cells (cell density 0.33×10^6 cells per mL) were seeded in a 10-L bioreactor. $p(O_2)$ (50% air saturation), temperature (27 °C), and stirring (80 rpm) were controlled. The culture was infected (1.1×10^6 cells per mL) with recombinant baculovirus containing a coding region for human purple acid phosphatase (MOI = 0.001).[31, 34] After six days the suspension was centrifuged (10 min, 5000 *g*) to remove the cells and the supernatant was used for purification.

Purification of recHPAP: Phosphocellulose (P11) was added to the supernatant (1 g per 200 U of enzyme activity), and the suspension was stirred at room temperature. If negligible activity remained in the supernatant, the P11 was allowed to settle, filtered, washed with buffer A (50 mM MES (pH 6.5), 0.1 M KCl), resuspended in 250 mL buffer B (50 mM MES (pH 6.5), 2 M KCl) and stirred at 4 °C overnight. The P11 was removed by filtration. (NH$_4$)$_2$SO$_4$ was added to the P11 filtrate (25% saturation, 34 g), and the suspension was stirred for 2 h at 4 °C. The suspension was centrifuged (15 min, 10 000 *g*) and the supernatant was loaded overnight onto a CL-4B phenyl-sepharose column (2.5 × 15 cm) preequilibrated with buffer C (50 mM MES (pH 6.5), 25% (w/v) (NH$_4$)$_2$SO$_4$, 0.25 M KCl). After washing (50 mL), a 100-mL linear gradient (25→0% (NH$_4$)$_2$SO$_4$) was applied to the column to elute the protein. Fractions containing recHPAP with *R* values (A_{280}/A_{520}) lower than 30 were pooled and concentrated on an Amicon ultrafiltration unit (YM 30 membrane). The concentrated sample was diluted and concentrated several times to a KCl concentration of 0.1 M, and applied onto a SP-Sepharose column (1.6 × 4 cm) preequilibrated with buffer A. A 20-mL gradient to buffer B was applied to elute the protein. Fractions with *R* < 18 were pooled and concentrated, reduced (5 mM (NH$_4$)$_2$Fe(SO$_4$)$_2$, 25 mM ascorbic acid, 3 min), and applied onto a HR10/30 Superose 12 column. After elution with buffer B, the reduced enzyme (*R* = 16) was stored at −20 °C.

Enzyme kinetics: Enzyme assays were performed by monitoring the formation of the *p*-nitrophenolate anion at 410 nm. The activity during purification was measured in a buffer (100 mM MES (pH 6.0), 300 mM KCl, 10 mM Na-K tartrate, 17.5 mM Na ascorbate, 0.37 mM $(NH_4)_2Fe(SO_4)_2)$ and 20–40 mM *p*-NPP at 22 °C. At several times after enzyme addition, aliquots (250 μL) were removed and quenched (1.0 mL, 0.5 M NaOH) to convert all product to the phenolate form ($\varepsilon_{410} = 16.6$ mM^{-1} cm^{-1}).

The pH dependence of k_{cat} for recHPAP was measured over the pH range 4 to 8 (100 mM buffer (NaOAc, MES, or HEPES), 10 mM Na-K tartrate, 300 mM KCl, 6.7 mM Na ascorbate, 0.37 mM $(NH_4)_2Fe(SO_4)_2)$ with different *p*-NPP concentrations (0.5 and 50 mM). For each determination of V_{max} and K_M, the hydrolysis rate was measured at eight different *p*-NPP concentrations. After each assay the pH value of the reaction mixture was measured to ensure that the pH of the solution had not changed. Values of K_M and V_{max} were obtained by nonlinear regression fits to the Michaelis–Menten equation, using the program EnzymeKinetics, version 1.4 (Trinity Software, Plymouth, NH, USA).

Proteolytic digestion with trypsin: Trypsin (0.035 mol per mole of PAP) was added to a sample of recHPAP (50 mM MES, pH 6.5, 2 M KCl), the sample was incubated at room temperature for 20 h, and specific activity was monitored over time. The sample was then diluted/concentrated several times by using a Centricon tube (cut-off 30 kDa) to remove the trypsin. After reduction (0.5 mM $(NH_4)_2Fe(SO_4)_2$, 17 mM ascorbic acid, 3 min), the sample was applied onto a HR10/30 Superose 12 column and eluted with buffer B, resulting in cleaved protein with $\lambda_{max} = 520$ nm. The cleaved protein obtained by this procedure was used for kinetics and spectroscopic measurements.

To follow cleavage by EPR, trypsin (0.035 mol per mole of PAP) was added to recHPAP (300 μL, 70 μM) in buffer D (50 mM NaOAc (pH 5.0), 2 M KCl), and the sample was immediately frozen in liquid N$_2$. After measuring its EPR spectrum at 4.3 K, the sample was thawed, and buffer exchanged to buffer B in two concentration/dilution steps by using a Centricon tube (cut-off 10 kDa) to initiate the proteolysis reaction. After incubation for the desired time, the buffer was again exchanged to buffer D to stop the proteolysis reaction. Before freezing in liquid N$_2$ for measurement of a second EPR spectrum, the enzymatic activity was measured and the PAP concentration was determined by visible absorption spectroscopy. This process was repeated with the same sample in order to obtain data points at longer incubation periods. Control experiments showed no change in activity or EPR spectrum in the absence of trypsin.

CD spectroscopy: Samples were prepared by buffer exchange of concentrated recHPAP samples (50 mM TRIS (pH 6.3), 150 mM KCl buffer). The concentrated samples were diluted to 0.100 mg mL^{-1} in the same buffer and immediately frozen (−80 °C) for transport. The sample was thawed and centrifuged immediately before measuring its CD spectrum. The pH and recHPAP concentration were checked after the spectrum was obtained. Data were analyzed with the program CONTIN (part of the software package STRUCTURE, which can be obtained from K. S. Vassilenko, Group of Protein Spectroscopy, Institute of Protein Research, Pushchino, Russia), and the results of three different analysis methods (Provencher and Glöckner, Venyaminov, Sreerama and Woody)[35–39] were averaged to give the final amounts of α-helix, β-sheet and -turn, and random-coil content.

Mass spectrometry and C- and N-terminal sequence analysis: Cleaved recHPAP was denatured (7 M guanidine hydrochloride/0.3 M TRIS, pH 9) and the disulfide bond was reduced with freshly prepared DTT solution (20 mM, 1:100 molar ratio, 1 h, 60 °C). The reduced fragments were separated on a reversed-phase HPLC column (C$_8$,

2.1 × 100 mm, 5 μm), installed on the SMART system, with a predefined gradient from solvent A (0.1 % TFA/milliQ-filtered water) to solvent B (0.08 % TFA/90 % acetonitrile/milliQ-filtered water): 0–60 min, 15–70 % B; 60–65 min, 70–100 % B; 65–72 min, 100 % B; 72–77 min, 100–15 % B. Fractions were collected in Eppendorf vials (500 μL).

C-terminal sequence analysis was performed by using a slightly modified chemical protocol from Boyd et al.[59] Prior to C-terminal sequence analysis, the protein was absorbed on a ProSorb sample preparation cartridge and, after subsequent washes with milliQ-filtered water, treated with phenylisocyanate under basic conditions to modify the lysine side chains.[60] The alkylated thiohydantoins were identified online by reversed-phase analysis with a linear gradient using solvent C (3.5 % THF/milliQ-filtered water/35 mM NaOAc, pH 3.8) and solvent D (100 % acetonitrile).

For nanoelectrospray mass spectrometry, a fraction of the RPLC eluate was dissolved (50 % acetonitrile/49.9 % milliQ-filtered water/ 0.1 % formic acid (v/v/v)) and loaded into a coated capillary which was then placed into the nanospray source delivered with the Q-TOF mass spectrometer. The needle was held at 1.3 kV while spray formation was initially stimulated by applying a low N$_2$ pressure at the back of the capillary. Spectra were taken from 600–2000 Da using 2-s scans and accumulated during 5 min. The obtained data were further processed with the MaxEnt software delivered with the instrument.

[1] E. V. Koonin, *Protein Sci.* **1994**, *3*, 356–368.
[2] J. B. Vincent, B. A. Averill, *FEBS Lett.* **1990**, *263*, 265–268.
[3] L. Que, Jr., A. E. True, *Prog. Inorg. Chem.* **1990**, *38*, 97–200.
[4] J. B. Vincent, G. L. Olivier-Lilley, B. A. Averill, *Chem. Rev.* **1990**, *90*, 1447–1467.
[5] D. E. Wilcox, *Chem. Rev.* **1996**, *96*, 2435–2458.
[6] T. Klabunde, B. Krebs, *Struct. Bonding (Berlin)* **1998**, *89*, 177–198.
[7] J. B. Vincent, B. A. Averill, *FASEB J.* **1990**, *4*, 3009–3014.
[8] D. F. Hunt, J. R. Yates, J. Shabanowitz, N. Z. Zhu, T. Zirino, B. A. Averill, S. T. Daurat-Larroque, J. G. Shewale, R. M. Roberts, K. Brew, *Biochem. Biophys. Res. Commun.* **1987**, *144*, 1154–1160.
[9] C. M. Ketcham, R. M. Roberts, R. C. M. Simmen, H. S. Nick, *J. Biol. Chem.* **1989**, *264*, 557–563.
[10] D. K. Lord, N. C. P. Cross, M. A. Bevilacqua, S. H. Rider, P. A. Gorman, A. V. Groves, D. W. Moss, D. Sheer, T. M. Cox, *Eur. J. Biochem.* **1990**, *189*, 287–293.
[11] E. Sinn, C. J. O'Connor, J. de Jersey, B. Zerner, *Inorg. Chim. Acta* **1993**, *78*, L13-L15.
[12] P. G. Debrunner, M. P. Hendrich, J. de Jersey, D. T. Keough, J. T. Sage, B. Zerner, *Biochim. Biophys. Acta* **1983**, *745*, 103–106.
[13] J. C. Davis, B. A. Averill, *Proc. Natl. Acad. Sci. USA* **1982**, *79*, 4623–4627.
[14] M. Merkx, B. A. Averill, *Biochemistry* **1998**, *37*, 11 223–11 231.
[15] J. L. Beck, D. T. Keough, J. de Jersey, B. Zerner, *Biochim. Biophys. Acta* **1984**, *791*, 357–363.
[16] R. C. Holz, L. Que, Jr., L.-J. Ming, *J. Am. Chem. Soc.* **1992**, *114*, 4434–4436.
[17] D. T. Keough, D. A. Dionysius, J. de Jersey, B. Zerner, *Biochem. Biophys. Res. Commun.* **1980**, *94*, 600–605.

[18] M. Merkx, B. A. Averill, *Biochemistry* **1998**, *37*, 8490 – 8497.

[19] M. Merkx, B. A. Averill, *J. Am. Chem. Soc*. **1999**, *121*, 6683 – 6689.

[20] N. Sträter, T. Klabunde, P. Tucker, H. Witzel, B. Krebs, *Science* **1995**, *268*, 1489 – 1492.

[21] C. R. Kissinger, H. E. Parge, D. R. Knighton, C. T. Lewis, L. A. Pelletier, A. Tempczyk, V. J. Kalish, K. D. Tucker, R. E. Showalter, E. W. Moomaw, L. N. Gastinel, N. Habuka, X. Chen, F. Maldonado, J. E. Barker, R. Bacquet, J. E. Villafranca, *Nature* **1995**, *378*, 641 – 644.

[22] J. P. Griffith, J. L. Kim, E. E. Kim, M. D. Sintchak, J. A. Thomson, M. J. Fitzgibbon, M. A. Fleming, P. R. Caron, K. Hsiao, M. A. Navia, *Cell* **1995**, *82*, 507 – 522.

[23] J. Goldberg, H.-B. Huang, Y.-G. Kwon, P. Greengard, A. C. Nairn, J. Kuriyan, *Nature* **1995**, *376*, 745 – 753.

[24] M. P. Egloff, P. T. W. Cohen, P. Reinemer, D. Barford, *J. Mol. Biol*. **1995**, *254*, 942 – 959.

[25] J. Uppenberg, F. Lindqvist, C. Svensson, B. Ek-Rylander, G. Andersson, *J. Mol. Biol*. **1999**, *290*, 201 – 211.

[26] L. W. Guddat, A. S. McAlpine, D. Hume, S. Hamilton, J. de Jersey, J. L. Martin, *Structure* **1999**, *7*, 757 – 767.

[27] Y. Lindqvist, E. Johansson, H. Kaija, P. Vihko, G. Schneider, *J. Mol. Biol*. **1999**, *291*, 135 – 147.

[28] J. L. Orlando, T. Zirino, B. J. Quirk, B. A. Averill, *Biochemistry* **1993**, *32*, 8120 – 8129.

[29] J. Ljusberg, B. Ek-Rylander, G. Andersson, *Biochem. J*. **1999**, *343*, 63 – 69.

[30] H. Kaija, J. Jia, Y. Lindqvist, G. Andersson, P. Vihko, *J. Bone Min. Res*. **1999**, *14*, 424 – 430.

[31] K. Marshall, K. Nash, G. Haussman, I. Cassady, D. Hume, J. de Jersey, S. Hamilton, *Arch. Biochem. Biophys*. **1997**, *345*, 230 – 236.

[32] M. M. Bradford, *Anal. Biochem*. **1976**, *72*, 248 – 254.

[33] U. K. Laemmli, *Nature* **1970**, *227*, 680 – 685.

[34] A. R. Hayman, T. M. Cox, *J. Biol. Chem*. **1994**, *269*, 1294 – 1300.

[35] J. T. Yang, C.-S. C. Wu, H. M. Martinez, *Meth. Enzymol*. **1986**, *130*, 208 – 269.

[36] Y. S. Venyaminov, I. A. Baikalov, Z. M. Shen, C.-S. C. Wu, J. T. Yang, *Anal. Biochem*. **1991**, *198*, 250 – 255.

[37] Y. S. Venyaminov, I. A. Baikalov, Z. M. Shen, C.-S. C. Wu, J. T. Wang, *Anal. Biochem*. **1993**, *214*, 17 – 24.

[38] S. W. Provencher, J. Glöckner, *Biochemistry* **1981**, *20*, 33 – 37.

[39] P. Manavalan, W. C. J. Johnson, *Anal. Biochem*. **1987**, *167*, 76 – 85.

[40] J. B. Vincent, M. W. Crowder, B. A. Averill, *Biochemistry* **1991**, *30*, 3025 – 3034.

[41] I. H. Segel, *Enzyme Kinetics: Behaviour and analysis of rapid equilibrium and steady-state enzyme systems*, Wiley, New York, **1993**, Chap. 11.

[42] M. Merkx, M. W. H. Pinkse, B. A. Averill, *Biochemistry* **1999**, *38*, 9914 – 9925.

[43] B. C. Antanaitis, P. Aisen, H. R. Lilienthal, R. M. Roberts, F. W. Bazer, *J. Biol. Chem*. **1980**, *255*, 11 204 – 11 209.

[44] B. Ek-Rylander, T. Barkhem, J. Ljusberg, L. Ohman, K. K. Andersson, G. Andersson, *Biochem. J*. **1997**, *321*, 305 – 311.

[45] B. C. Antanaitis, P. Aisen, *J. Biol. Chem*. **1982**, *257*, 1855 – 1859.

[46] M. W. Crowder, J. B. Vincent, B. A. Averill, *Biochemistry* **1992**, *31*, 9603 – 9608.

[47] B. C. Antanaitis, P. Aisen, *J. Biol. Chem*. **1982**, *257*, 5330 – 5332.

[48] B. A. Averill, J. C. Davis, S. Burman, T. Zirino, J. Sanders-Loehr, T. M. Loehr, J. T. Sage, P. G. Debrunner, *J. Am. Chem. Soc*. **1987**, *109*, 3760 – 3767.

[49] M. A. S. Aquino, J.-S. Lim, A. G. Sykes, *J. Chem. Soc. Dalton Trans*. **1994**, *4*, 429 – 436.

[50] M. Dietrich, D. Münstermann, H. Suerbaum, H. Witzel, *Eur. J. Biochem*. **1991**, *199*, 105 – 113.

[51] B. C. Antanaitis, T. Strekas, P. Aisen, *J. Biol. Chem*. **1982**, *257*, 3766 – 3770.

[52] B. C. Antanaitis, P. Aisen, H. R. Lilienthal, *J. Biol. Chem*. **1983**, *258*, 3166 – 3172.

[53] J. Zhang, Z. J. Zhang, K. Brew, E. Y. C. Lee, *Biochemistry* **1996**, *35*, 6276 – 6282.

[54] P. Mertz, L. Yu, R. Sikkink, F. Rusnak, *J. Biol. Chem*. **1997**, *272*, 21 296 – 21 302.

[55] S. Zhuo, J. C. Clemens, R. L. Stones, J. E. Dixon, *J. Biol. Chem*. **1994**, *269*, 26 234 – 26 238.

[56] A. Mondragon, E. C. Griffith, L. Sun, F. Xiong, C. Armstrong, J. O. Liu, *Biochemistry* **1997**, *36*, 4934 – 4942.

[57] R. H. Hoff, P. Mertz, F. Rusnak, A. C. Hengge, *J. Am. Chem. Soc*. **1999**, *121*, 6382 – 6390.

[58] H. B. Huang, A. Horiuchi, J. Goldberg, P. Greengard, A. C. Nairn, *Proc. Natl. Acad. Sci. USA* **1997**, *94*, 3530 – 3535.

[59] V. L. Boyd, M. Bozzini, G. Zon, R. L. Noble, B. Mattaliano, *Anal. Biochem*. **1992**, *206*, 344 – 352.

[60] M. Bozzini, J. Zhao, P.-M. Yuan, P. Ciolek, Y.-C. Pan, J. Horton, D. R. Marshak, V. L. Boyd in *Techniques in Protein Chemistry, Vol. VI* (Ed.: J. Crabb), Academic Press, London, **1995**, pp. 229 – 237.

[61] B. Samyn, K. Hardeman, J. Van der Eycken, J. Van Beeumen, *Anal. Chem*. **2000**, *72*, 1389 – 1399.

[62] A. R. Hayman, M. J. Warburton, J. A. S. Pringle, B. Coles, T. J. Chambers, *Biochem. J*. **1989**, *261*, 601 – 609.

[63] R. A. Sayle, E. J. Milner-White, *Trends Biochem. Sci*. **1995**, *20*, 374.

[64] Abbreviations: BSPAP = bovine spleen purple acid phosphatase, DTT = dithiothreitol, HEPES = *N*-(2-hydroxyethyl)piperazine-*N'*-(2-ethanesulfonic acid), KBPAP = kidney bean purple acid phosphatase, MES = 2-(*N*-morpholino)ethanesulfonic acid, MOI = multiplicity of infection, PAP = purple acid phosphatase; *p*-NPP = *para*-nitrophenylphosphate, PP1 = protein phosphatase 1, PP2B = calcineurin, recHPAP = recombinant human purple acid phosphatase, recHPAP$_{cleaved,ox}$ = cleaved oxidized rec-HPAP, recHPAP$_{cleaved,red}$ = cleaved mixed-valent recHPAP, recHPAP$_{mono,ox}$ = monomeric oxidized recHPAP, recHPAP$_{mono,red}$ = monomeric mixed-valent recHPAP, recRPAP = recombinant rat bone purple acid phosphatase, Sf9 cells = cells from *Spodoptera frugiperda*, TFA = trifluoroacetic acid, TRAP = tartrate-resistant acid phosphatase, TRIS = tris(hydroxymethyl)-aminomethane, Uf = uteroferrin.